Strong influence of El Niño Southern Oscillation on flood risk around the world

Philip J. Ward[a,b,1], Brenden Jongman[a,b], Matti Kummu[c], Michael D. Dettinger[d,e], Frederiek C. Sperna Weiland[f], and Hessel C. Winsemius[f]

[a]Institute for Environmental Studies and [b]Amsterdam Global Change Institute, VU University Amsterdam, 1081 HV Amsterdam, The Netherlands; [c]Water and Development Research Group, Aalto University, 02150 Espoo, Finland; [d]Climate Atmospheric Sciences and Physical Oceanography Division, Scripps Institution of Oceanography, La Jolla, CA 92093; [e]United States Geological Survey, La Jolla, CA 92093; and [f]Deltares, 2629 HD Delft, The Netherlands

Edited by Peter H. Gleick, Pacific Institute for Studies in Development, Environment, and Security, Oakland, CA, and approved September 22, 2014 (received for review May 27, 2014)

El Niño Southern Oscillation (ENSO) is the most dominant interannual signal of climate variability and has a strong influence on climate over large parts of the world. In turn, it strongly influences many natural hazards (such as hurricanes and droughts) and their resulting socioeconomic impacts, including economic damage and loss of life. However, although ENSO is known to influence hydrology in many regions of the world, little is known about its influence on the socioeconomic impacts of floods (i.e., flood risk). To address this, we developed a modeling framework to assess ENSO's influence on flood risk at the global scale, expressed in terms of affected population and gross domestic product and economic damages. We show that ENSO exerts strong and widespread influences on both flood hazard and risk. Reliable anomalies of flood risk exist during El Niño or La Niña years, or both, in basins spanning almost half (44%) of Earth's land surface. Our results show that climate variability, especially from ENSO, should be incorporated into disaster-risk analyses and policies. Because ENSO has some predictive skill with lead times of several seasons, the findings suggest the possibility to develop probabilistic flood-risk projections, which could be used for improved disaster planning. The findings are also relevant in the context of climate change. If the frequency and/or magnitude of ENSO events were to change in the future, this finding could imply changes in flood-risk variations across almost half of the world's terrestrial regions.

flood risk | El Niño Southern Oscillation | climate variability | global scale | flood hazard

El Niño Southern Oscillation (ENSO) is the most dominant interannual signal of climate variability on Earth (1) and influences climate over large parts of the Earth's surface. In turn, ENSO is known to strongly influence many physical processes and societal risks, including droughts, food production, hurricane damage, and tropical tree cover (2–4). For decision makers it is essential to have information on the possible impacts of this climate variability on society. Such information can be particularly useful when the climate variability can be anticipated in advance, thus allowing for early warning and disaster planning (5). For example, projections carried out in September 2013 already suggested a 75% likelihood that El Niño conditions would develop in late 2014 (6). According to the ENSO forecast of the International Research Institute for Climate and Society and the Climate Prediction Center/NCEP/NWS, dated 9 October 2014, observed ENSO conditions did indeed move to those of a borderline El Niño during September and October 2014, with indications of weak El Niño conditions during the northern hemisphere winter 2014–2015 (iri.columbia.edu/our-expertise/climate/forecasts/enso/current/).

However, to date little is known on ENSO's influence on flood risk, whereby risk is defined as a function of hazard, exposure, and vulnerability (7) and is expressed in terms of socioeconomic indicators such as economic damage or affected people. Although global-scale flood-risk assessments have recently become a hot topic in both the scientific and policy communities, assessments to date have focused on current risks (7–11) or future risks under long-term mean climate change (12, 13). Meanwhile, other recent research suggests that ENSO-related variations of precipitation are likely to intensify in the future (14, 15) and that extreme El Niño events may increase in frequency (16). Hence, an understanding of ENSO's influence on flood risk is vital in understanding both the possible impacts of upcoming ENSO events as well as planning for the potential socioeconomic impacts of changes in future ENSO frequency.

In this paper, we show for the first time to our knowledge that ENSO has a very strong influence on flood risk in large parts of the world. These findings build on previous studies, especially in Australia and the United States, which show that ENSO and other forms of climate variability are strongly related to flood hazard in some regions (17–25). To do this, we developed a modeling framework to specifically assess ENSO's influence on global flood risk. The modeling framework involves using a cascade of hydrological, hydraulic, and impact models (10, 11). Using this model cascade, we assessed flood impacts in terms of three indicators: (*i*) exposed population, (*ii*) exposed gross domestic product (GDP), and (*iii*) urban damage (*Materials and Methods*). A novel aspect of the framework is that we are able to calculate flood risk conditioned on the climatology of all years, El Niño years only, and La Niña years only. This allows us, for the first time to our knowledge, to simulate the impacts of ENSO

Significance

El Niño Southern Oscillation (ENSO) affects hydrological processes around the globe. However, little is known about its influence on the socioeconomic impacts of flooding (i.e., flood risk). We present, to our knowledge, the first global assessment of ENSO's influence on flood risk in terms of economic damage and exposed population and gross domestic product. We show that reliable flood risk anomalies exist during ENSO years in basins spanning almost half of Earth's surface. These results are significant for flood-risk management. Because ENSO can be predicted with lead times of several seasons with some skill, the findings pave the way for developing probabilistic flood-risk projections. These could be used for improved disaster planning, such as temporarily increasing food and medicine stocks by relief agencies.

Author contributions: P.J.W., M.K., M.D.D., and H.C.W. designed research; P.J.W., B.J., F.C.S.W., and H.C.W. performed research; P.J.W. and H.C.W. analyzed data; and P.J.W., B.J., M.K., M.D.D., and H.C.W. wrote the paper.

The authors declare no conflict of interest.

This article is a PNAS Direct Submission.

Freely available online through the PNAS open access option.

[1]To whom correspondence should be addressed. Email: philip.ward@ivm.vu.nl.

This article contains supporting information online at www.pnas.org/lookup/suppl/doi:10.1073/pnas.1409822111/-/DCSupplemental.

on flood risk. The hydrological and impact models have previously been validated for the period 1958–2000 (11). Here, we carried out further validation to assess the specific ability of the model cascade to simulate year-to-year fluctuations in peak river flows and flood impacts and anomalies in peak flows and impacts during El Niño and La Niña years (*SI Discussion, Validation of Hydrological and Hydraulic Models*).

Anomalies in Flood Hazard at the Global Scale

We show that significant anomalies in flood volumes (compared with all years) exist across more than a third of the Earth's land surface (excluding Greenland and Antarctica) during both El Niño and La Niña years, namely 34% during El Niño years and 38% during La Niña years (Fig. 1). In Fig. 1, we show significant anomalies in flood volumes with a return period of 100 y. Statistical significance per cell was assessed by bootstrapping the anomalies ($\alpha = 0.05$, 1,000 repetitions). Field significance of the gridded results was assessed using the binomial distribution (26) and found to be highly significant ($P < 0.001$). In some arid regions, the anomaly in flood volumes is relatively small in absolute terms yet statistically significant. Therefore, in Fig. S1 we also show the absolute anomalies in flood volumes. We also examined anomalies in flood volumes for different return periods, ranging from 5 to 1,000 y (Figs. S2 and S3). The patterns of the anomalies remain similar across different return periods. In *SI Discussion, Validation of Hydrological and Hydraulic Models* we describe the validation of the hydrological and hydraulic models in terms of their ability to simulate relative differences in peak annual discharge between different ENSO phases. Relative differences in simulated extreme discharge between the different ENSO phases are generally simulated well. However, in northern high-latitude regions and parts of Central America correlation of annual maximum discharge between years is relatively low.

A few previous studies have examined ENSO's influence on flood-hazard-related variables in specific region (17–21, 24, 25), especially the United States and Australia, and a comparison between our results and those studies is found in SI Text (*SI Discussion, Comparison with Past Results*). Moreover, relationships have been found globally between ENSO and annual peak discharges (27, 28), but to date no such global scale analysis has been carried out for flood hazard.

Anomalies in Flood Risk at the Globally Aggregated Scale

Next, we examined the influence of ENSO on flood risk at the globally aggregated scale. First, we assessed the correlation (Spearman's) between globally aggregated impacts and the Japan Meteorological Agency's Sea Surface Temperature (JMA SST) anomaly index of ENSO per year (*Materials and Methods*). At this aggregated scale we found no statistically significant correlation for any of the impact indicators (i.e., exposed population, exposed GDP, and urban damage) (Table 1). We also assessed flood risk in terms of annual expected impacts. The

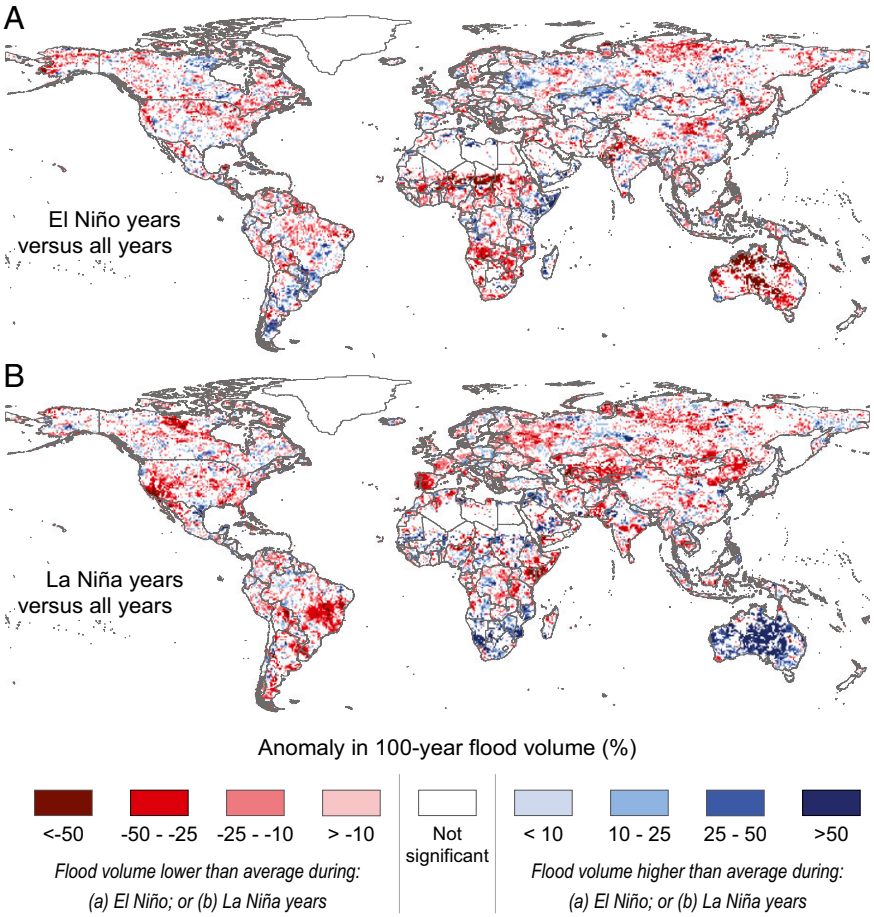

Fig. 1. Percentage anomaly in flood volumes with return periods of 100 y during (*A*) El Niño years and (*B*) La Niña years (compared with all years). Statistical significance per cell was assessed by bootstrapping ($\alpha = 0.05$), using 1,000 repetitions. Field significance of the gridded results was assessed using the binomial distribution (26) and found to be highly significant ($P < 0.001$). Absolute values of the flood anomalies (normalized to area) are shown in Fig. S1. For validation results see *SI Discussion, Validation of Hydrological and Hydraulic Models*.

Table 1. Flood impact results aggregated to the global scale

	Flood risk indicator		
	Exposed population	Exposed GDP	Urban damage
Correlation between impacts per hydrological year and JMA SST_{DJF}			
Rho	−0.14	0.21	0.25
P	0.36	0.18	0.11
Anomalies in annual expected impacts			
El Niño years, %	−8.7	−6.2	−6.8
La Niña years, %	−6.0	−10.2	−14.2

Table shows the correlation (Spearman's rank, rho) between simulated impacts per hydrological year and the JMA SST anomaly index for December–February (JMA SST_{DJF}) and percentage anomalies in simulated annual expected impacts for El Niño and La Niña years (compared with all years).

absolute values based on all years are 154 million people for annual exposed population, $1 trillion [purchasing power parity (PPP)] for annual exposed GDP and $900 billion (PPP) for annual expected urban damage. Compared with these, we found negative anomalies (i.e., lower risk) during both El Niño and La Niña years for all indicators (Table 1). Nevertheless, none of these differences was found to be reliable. Here, reliability refers to whether the annual expected impact at 5th and 95th percentile fits of the Gumbel distribution for El Niño years (or La Niña years) falls outside the range of the corresponding 5th and 95th percentile fits for annual expected impacts from all years (*Materials and Methods*).

These findings are in line with several studies examining relationships between ENSO and flood disasters based on globally aggregated reported loss data. A study of the globally aggregated number of people affected by floods according to the EM-DAT Disaster Events database (29) found no significant correlation with an index of ENSO. Similarly, two studies examining possible relationships between global disaster frequency and ENSO, using data from the US Agency for International Development's Office (30) and EM-DAT (31), found no significant difference between neutral years and El Niño years. It should be noted that the latter study looked at all hydro-meteorological disasters, not just flooding (31), and that the former study only examined El Niño years (not La Niña years) (30).

Anomalies in Flood Risk at the Regional Scale

However, the modeling framework developed here allows us to move beyond globally aggregated results and examine spatially differentiated ENSO influences on flood risk. Regional anomalies in expected annual urban damage in El Niño and La Niña years are shown in Fig. 2, at the scale of food-producing units (FPUs) (32), units that represent a hybrid of countries and river basins. There are differences in the strength and patterns of ENSO influences between the results for urban damage (Fig. 2), exposed GDP (Fig. S4), and exposed population (Fig. S5). These differences are discussed in *SI Discussion*, *Main Differences in Results Between Indicators* and summarized in Table S1. Here, we focus the discussion on the results for urban damage, although it should be noted that for exposed GDP and exposed population there are even more areas with large, reliable anomalies.

Reliable anomalies in expected urban damage exist in at least one ENSO phase (El Niño or La Niña, or both) in FPUs covering 44% of Earth's land area (Fig. 3*A*). At the scale of individual FPUs, the results show particularly strong anomalies in southern Africa, parts of the Sahel and western Africa, Australia, the western United States (especially during La Niña anomalies), and parts of South America (Fig. 2). Strong anomalies were also simulated in parts of Central Eurasia (especially during El Niño), although it should be noted that the validation results show that the model cascade is less reliable in this region (*SI Discussion*, *Validation of Hydrological and Hydraulic Models*).

It is important to note that El Niño and La Niña are associated with both positive and negative anomalies in risk (depending on location and phase). Our simulations revealed reliable anomalies in annual expected urban damage during El Niño years for regions covering 29% of the Earth's land surface, with increased urban damage for 10% and decreased damage for 19%. During La Niña years we simulated reliable anomalies across 23% of the Earth's land surface, with increased damage for 10% and decreased damage for 13%. There are very few areas in which risk is lower during both ENSO phases (<0.1% of land area) or higher during both ENSO phases (<0.1%). We find that asymmetries in annual expected urban damage between ENSO phases are the norm, so that anomalies in annual expected urban damages only switched sign from one ENSO phase (e.g., El Niño) to the other (e.g., La Niña) in FPUs covering 7% of Earth's land surface. If we restrict the analysis only to FPUs with large ENSO-related urban damage anomalies (i.e., anomalies exceeding 25%) we still find ENSO influences in basins covering 40% of the Earth's land surface (Fig. 3*B*). As with the full range of anomalies, we find few areas in which these large anomalies have opposite signs in the two ENSO phases (5%). However, there is a large difference between the total land area with negative anomalies in one ENSO phase and no anomaly in the other phase (26%) vs. those with positive anomalies in one ENSO phase and no anomaly in the other (9%).

Discussion

The results show that for risk assessments it is vital to consider both the positive and negative anomalies in risk associated with ENSO. Reporting of ENSO impacts in the media tends to only focus on its negative effects (see also ref. 31). This may partly explain why a past study on the reported frequency of flood disasters only found significant relationships with ENSO in a handful of countries (30), because that study only examined countries in which disaster frequency was higher during El Niño years and not those where it was lower. Our results thus call for more balanced assessments of ENSO impacts to identify both possible negative and positive affects for society and the economy.

Thus, flood risks associated with ENSO (and, presumably, other global modes of climate variation) show strong, complicated, and societally significant patterns at spatial scales well below that of global aggregations. Indeed, the aggregation scale used to represent anomalies in risk strongly affects the findings. A comparison of anomalies in annual expected flood damage at the country scale (Fig. S6) with those at the FPU scale (Fig. 2) reveals that country-scale assessments mask important regional ENSO influences on risk, especially in large countries where there are subregions that exhibit opposing ENSO influences, such as the United States and Australia. Country-aggregated results indicate no reliable anomaly in the United States during El Niño or La Niña years (Fig. S6), but the regionally (FPU-) disaggregated influences rise to high levels (Fig. 2). Our spatially distributed modeling approach allows us to capture such regional influences in risk, which is not possible using global-scale databases of reported disaster events or losses, because these tend to only list events per country, or at best rudimentary indications of location.

These findings are also relevant to considerations of changing flood risks under a changing climate. Many studies have shown that the frequency and/or intensity of ENSO has varied widely during past millennia to decades (33–36). Our work suggests that such changes in ENSO frequency or intensity, if they recurred in today's world, could have large impacts on flood risk in many regions. Although there is currently no agreement between climate models as to how the frequency of ENSO will change as a result of global warming (37–39), ENSO-related interannual variations of sea-surface temperatures and precipitation are likely to intensify in the future (14, 15), and recent research shows that

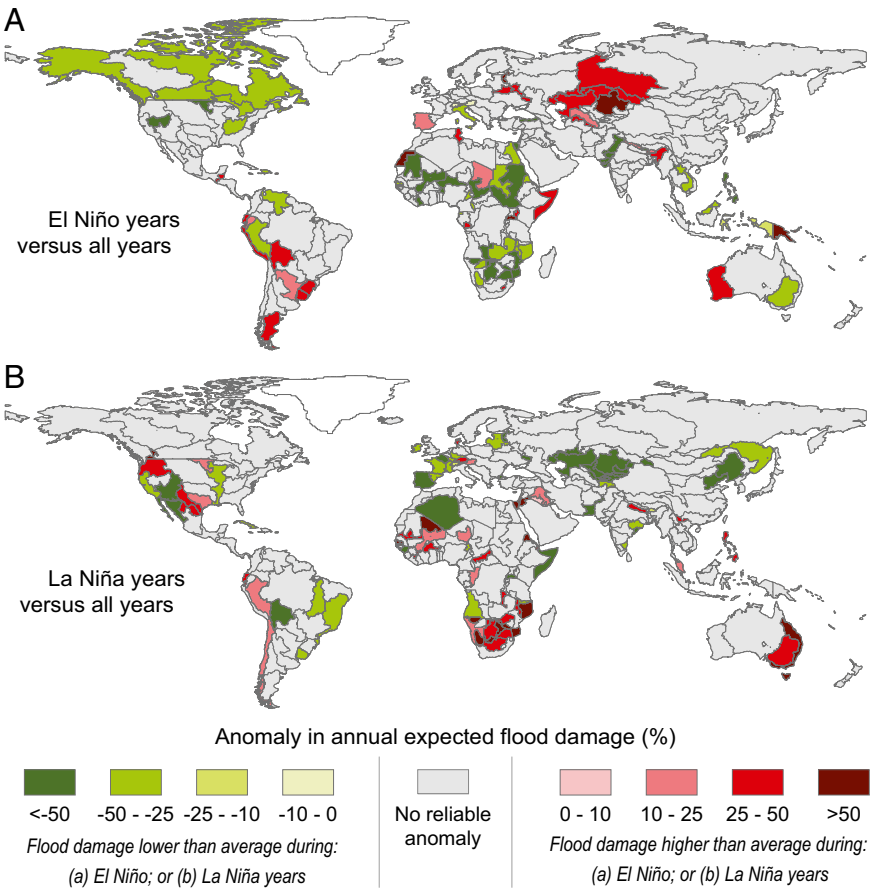

Fig. 2. Percentage anomaly per FPU in annual expected damage in urban areas during (*A*) El Niño years and (*B*) La Niña years (compared with all years). Similar results for annual exposed GDP and annual exposed population are shown in Figs. S4 and S5, respectively. For validation results see *SI Discussion, Validation of Impact Assessment Results*.

extreme El Niño events may increase in frequency (16). If so, given the relationships between ENSO and flood hazard reported here we would anticipate increases in flood risk variability across many, or indeed almost half, of the world's terrestrial regions in the future.

This study is a first attempt to simulate the influence of ENSO on flood risk at the global scale in terms of socioeconomic impacts. We have carried out analyses of the statistical significance in the anomalies in flood volumes and assessed the reliability of the anomalies in risk. The uncertainty of Global Flood Risk with IMAGE Scenarios modeling chain (GLOFRIS) associated with the use of different climate-forcing data and the extrapolation of the extreme value analyses to derive flood volumes up to return periods of 1,000 y has been assessed in ref. 11. Future studies should also attempt to perform full uncertainty analyses. This would require a Monte Carlo-based approach, in which each part of the modeling chain would be rerun with large sets (e.g., 1,000) of different parameter values. This would require the simulation of tens to hundreds of thousands of global flood inundation maps. At the global scale this is not feasible with current computing power. However, in those regions where ENSO impacts on flood risk have been identified more local studies could help to refine our findings and would allow for such full uncertainty assessments.

The implications for risk management are manyfold. For example, the findings have proven useful for the reinsurance industry. In those regions where disaster risk is strongly influenced by ENSO, the spatial and temporal variability in flood risk means that the likelihood of damage claims may increase (or decrease) in particular ENSO phases, affecting the financial resources that need to be reserved to cover losses. It also means that optimal premiums may vary through time, especially in regions where flood damages show strong spatial coherence between nearby basins (40). Moreover, the potential predictability of ENSO (6, 41) might be harnessed to try to account for short-term changes in loss probabilities (42). The findings are also of use to humanitarian institutions. Although humanitarian institutions were established to respond to disasters, there is an increasing discourse on the usefulness of ex-ante actions, especially since the signing of the Hyogo Framework for Action (43). ENSO-based forecasts of increased flood impacts with seasonal lead times could allow for preparatory risk reduction actions to be taken. For example, based on seasonal forecasting of above-normal rainfall in 2008 the International Federation of Red Cross and Red Crescent Societies' regional office in West Africa was able to presource disaster management supplies ahead of time, thereby improving supply availability from about 40 d to 2 d when floods occurred (44). However, this type of action is uncommon, because decision makers are often unable to translate the probability of seasonal above-normal rainfall into a meaningful evaluation in the change of flood or disaster risk (45). The findings from this study explicitly examine changes to such risk and can therefore be more directly translated into appropriate risk reduction actions in El Niño or La Niña years.

When designing actual measures, ideally risk analyses would be carried out for all localities using high-quality datasets, models, and expert knowledge on the ground. However, in practice the models and data required to carry out such analyses only exist in a few regions. In recent years, the value of global-scale risk models to fill this gap and to provide actionable information for flood risk reduction has been demonstrated (7, 46). Because they can provide

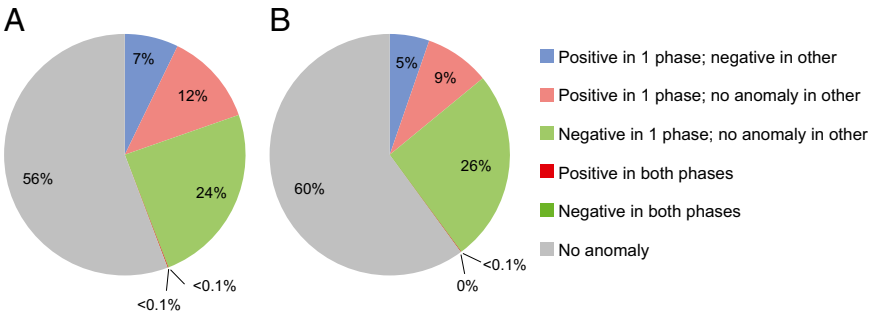

Fig. 3. Percentage of global land area (excluding Antarctica and Greenland) for which there are (*A*) reliable anomalies in annual expected urban damage during either/both El Niño and La Niña years and (*B*) reliable anomalies exceeding 25% in annual expected urban damage during either/both El Niño and La Niña years. For example, "positive in 1 phase; negative in other" means there is a reliable anomaly in either the El Niño or La Niña phase and a negative anomaly in the opposite phase.

information relatively rapidly and cheaply and use consistent methodologies and datasets across different geographical regions, global scale risk assessments can be used to assess the feasibility and prioritization of large-scale strategies before proceeding to local-scale studies.

Materials and Methods

The methods build upon the global flood risk assessment approach described in ref. 11. This approach uses a cascade of hydrological and hydraulic models (10, 11) to simulate inundation extent and depth (in decimeters) at a horizontal resolution of 30 × 30 arcseconds. Two kinds of inundation maps were simulated: (*i*) an inundation map for each hydrological year 1959–2000 and (*ii*) an inundation map for different return periods (5, 10, 25, 50, 100, 250, 500, and 1,000 y) conditioned on all years, El Niño years only, and La Niña years only. The inundation maps were combined with gridded data on urban density, population density, and GDP to estimate flood impacts (11).

More specifically, the method involves (*i*) hydrological and hydraulic modeling to develop daily time series of flood volumes, (*ii*) extreme value statistics to estimate flood volumes for different return periods, (*iii*) inundation modeling for different return periods, and (*iv*) impact modeling. Each step is described below.

Hydrological and Hydraulic Modeling. We simulated daily gridded discharge and flood volume at a horizontal resolution of 0.5° × 0.5° using PCR-GLOBWB-DynRout (47) forced by daily meteorological fields (precipitation, temperature, global radiation) for 1958–2000 from EU-WATCH (48). This procedure is described in ref. 11. This forcing dataset was used because it is the longest temporally consistent global reanalysis dataset currently available at this resolution. Validation of the peak annual discharge results is discussed in *SI Discussion, Validation of Hydrological and Hydraulic Models* and shown in Figs. S7 and S8.

Extreme Value Statistics. From the daily gridded flood volume time series we extracted an annual time series of maximum flood volumes for hydrological years 1959–2000. Here, hydrological years either refer to the period October–September (for most basins) or July–June (for basins in which the flood season occurs in the boreal autumn, i.e., September–November), following the method described in ref. 28. The hydrological years are referred to by the year in which they end, as per standard convention (i.e., hydrological year 1970 refers to the period October 1969 to September 1970). From this, we extracted time series for El Niño and La Niña years only, based on the ENSO classification of the Center for Ocean-Atmospheric Prediction Studies (coaps.fsu.edu/jma.shtml; Table 2). In the original dataset, ENSO years refer to the period October–September, whereby ENSO year 1970 refers to the period October 1970 to September 1971. These were therefore adjusted by 1 y to be consistent with the hydrological year naming convention. We then fit a Gumbel distribution through these three time series (all years, El Niño years, and La Niña years), based on nonzero data, extracting Gumbel parameters for the best-fit and 5th and 95th percentile confidence limits. These Gumbel parameters were then used to calculate flood volumes per grid cell for each return period and for each ENSO phase. Flood volumes were calculated conditioned on the exceedance probability of zero flood volume. For those cells where fewer than five nonzero data points were available in the entire series, flood volume was assumed to be zero.

Inundation Modeling. The coarse-resolution flood volume maps were converted into high-resolution (30- × 30-arcseconds) inundation maps using the GLOFRIS downscaling model (10, 11). First, inundation maps were simulated for each hydrological year (1959–2000) using the annual maps of flood volume from PCR-GLOBWB-DynRout as input. Second, inundation maps were simulated for each return period, conditioned on all years and on El Niño and La Niña years only using the flood volumes derived from the fitted extreme value statistics.

Impact Modeling. Each inundation map was combined with gridded socioeconomic data using the flood impact assessment module (11), which results in a high-resolution (30- × 30-arcseconds) map for each flood impact indicator, namely, exposed population, exposed GDP, and urban damage.

The data and methods used for each specific indicator are described in ref. 11, and in *SI Materials and Methods*. The gridded data can be aggregated to any geographical unit, given the corresponding shapefile. Here, we aggregated the results to the scale of countries and (adapted) FPUs (32), a hybrid of countries and river basins. The simulations produced maps showing impacts for each hydrological year (1959–2000) and also for the different return periods. Annual expected impacts were calculated as the area under an exceedance probability–impact (risk) curve where we assumed that the impact from a 2-y event is zero. Note that the method used assumes that no flood protection measures (e.g., dikes and retention areas that offer protection beyond the 2-y bankfull constraints) are in place. Although the assumption of the flood protection standard has a large influence on the absolute risk estimates (11), we found relative differences between ENSO phases to be fairly insensitive (Table S2). The impact results are validated against reported impacts in *SI Discussion, Validation of Impact Assessment Results* and summarized in Tables S3 and S4.

Statistical Analyses. We assessed correlation between annual hydrological year impacts and JMA SST anomaly index (JMA SST_{DJF}) using Spearman's rank. Significance was assessed by bootstrapping, using 1,000 repetitions. For anomalies in flood volumes between ENSO phases, statistical significance was assessed by bootstrapping the anomalies using 1,000 repetitions. For the annual expected impacts we simulated inundation maps for each return period based on all years, El Niño years, and La Niña years. For each of these we produced inundation maps based on the best fit and the 5th and 95th percentile confidence limits of the Gumbel distribution. We then used these as input to the impact module to estimate impacts for each return period

Table 2. Hydrological years categorized as El Niño and La Niña

ENSO mode	Hydrological year
El Niño	1964, 1966, 1970, 1973, 1977, 1983, 1987, 1988, 1992, 1998
La Niña	1965, 1968, 1971, 1972, 1974, 1975, 1976, 1989, 1999, 2000

Source: coaps.fsu.edu/jma.shtml. Other years are ENSO-neutral. Hydrological and ENSO year classifications are described in *Materials and Methods, Extreme Value Statistics*.

per ENSO phase and for each of the Gumbel fits. We then calculated annual expected impacts for each ENSO phase based on the three Gumbel fits. The anomaly in El Niño (or La Niña) years was calculated as a percentage relative to all years, based on the best-fit. We assessed the reliability of the anomaly based on whether annual expected impacts at 5th and 95th percentile fits for El Niño years (or La Niña years) fell outside the range in corresponding 5th and 95th percentile fits for annual expected impacts from all years. Anomalies in flood volumes per cell between ENSO phases were assessed by bootstrapping the anomalies ($\alpha = 0.05$, 1,000 repetitions). Field significance of the gridded results was assessed using the binomial distribution (26).

ACKNOWLEDGMENTS. We thank the editor and three anonymous reviewers for their valuable comments. We also thank Erin Coughlan (Red Cross/Red Crescent Climate Centre), Alanna Simpson (World Bank Global Facility for Disaster Reduction and Recovery), and Mark Guishard [Risk Prediction Initiative (RPI2.0)] for comments on, and input to, the manuscript. This research was funded by a Veni grant from the Netherlands Organisation for Scientific Research and by a research grant from the RPI2.0 of the Bermuda Institute of Ocean Sciences. Model validation was carried out in the framework of the ENHANCE project (Enhancing risk management partnerships for catastrophic natural hazards in Europe), funded by European Commission Grant 308438. M.K. received funding from Academy of Finland-funded project SCART Grant 267463 (Global green-blue water trajectories and measures for adaptation: linking the Holocene to the Anthropocene). M.D.D. received operational support from the California–Nevada Climate Applications Program, a US National Oceanic and Atmospheric Administration-funded Regional Integrated Science and Assessment program.

1. McPhaden MJ, Zebiak SE, Glantz MH (2006) ENSO as an integrating concept in earth science. *Science* 314(5806):1740–1745.
2. Cane MA, Eshel G, Buckland RW (1994) Forecasting Zimbabwean maize yield using eastern equatorial Pacific sea surface temperature. *Nature* 370:204–205.
3. Pielke RA, Jr, Landsea CN (1999) La Niña, El Niño, and Atlantic hurricane damages in the United States. *Bull Am Meteorol Soc* 80(10):2027–2033.
4. Holgren M, Hirota M, Van Nes EH, Scheffer M (2013) Effects of interannual climate variability on tropical tree cover. *Nat Climate Change* 3:755–758.
5. Coughlan de Perez E, Monasso F, Van Aalst M, Suarez P (2014) Science to prevent disasters. *Nat Geosci* 7:78–79.
6. Ludescher J, et al. (2014) Very early warning of next El Niño. *Proc Natl Acad Sci USA* 111(6):2064–2066.
7. UNISDR (2011) *Global Assessment Report on Disaster Risk Reduction. Revealing Risk, Redefining Development* (United Nations International Strategy for Disaster Reduction Secretariat, Geneva).
8. Jongman B, Ward PJ, Aerts JCJH (2012) Global exposure to river and coastal flooding: Long term trends and changes. *Glob Environ Change* 22(4):823–835.
9. Pappenberger F, Dutra E, Wetterhall F, Cloke H (2012) Deriving global flood hazard maps of fluvial floods through a physical model cascade. *Hydrol Earth Syst Sci* 16: 4143–4156.
10. Winsemius HC, Van Beek LPH, Jongman B, Ward PJ, Bouwman A (2013) A framework for global river flood risk assessments. *Hydrol Earth Syst Sci* 17:1871–1892.
11. Ward PJ, et al. (2013) Assessing flood risk at the global scale: Model setup, results, and sensitivity. *Environ Res Lett* 8(4):044019.
12. Hirabayashi Y, et al. (2013) Global flood risk under climate change. *Nat Clim Change* 3:816–821.
13. Arnell NW, Lloyd-Hughes B (2014) The global-scale impacts of climate change on water resources and flooding under new climate and socio-economic scenarios. *Clim Change* 122(1-2):127–140.
14. IPCC (2013) *Summary for Policymakers. Climate Change 2013: The Physical Science Basis. Contribution of Working Group I to the Fifth Assessment Report of the Intergovernmental Panel on Climate Change* (Cambridge Univ Press, Cambridge, UK).
15. Power S, Delage F, Chung C, Kociuba G, Keay K (2013) Robust twenty-first-century projections of El Niño and related precipitation variability. *Nature* 502(7472):541–545.
16. Cai W, et al. (2014) Increasing frequency of extreme El Niño events due to greenhouse warming. *Nat Clim Change* 4:111–116.
17. Cayan DR, Webb RH (1992) El Niño / Southern Oscillation and streamflow in the western United States. *El Niño: Historical and paleoclimatic aspects of the Southern Oscillation*, eds Diaz HF, Markgraf V (Cambridge Univ Press, Cambridge, UK), pp 29–68.
18. Cayan DR, Redmond KT, Riddle LG (1999) ENSO and hydrologic extremes in the western United States. *J Clim* 12:2881–2893.
19. Waylen PR, Caviedes CN (1986) El Niño and annual floods on the north Peruvian littoral. *J Hydrol (Amst)* 89:141–156.
20. Franks S (2002) Identification of a change in climate state using regional flood data. *Hydrol Earth Syst Sci* 6:11–16.
21. Kiem AS, Franks SW, Kuczera G (2003) Multi-decadal variability of flood risk. *Geophys Res Lett* 30(2):1035.
22. Micevski T, Franks SW, Kuczera GA (2006) Multidecadal variability in coastal eastern Australian flood data. *J Hydrol (Amst)* 327(1-2):219–225.
23. Pui A, Lal A, Sharma A (2011) How does the Interdecadal Pacific Oscillation affect design floods in Australia? *Water Resources Res* 47:W05554.
24. Kiem AS, Verdon-Kidd DC (2013) The importance of understanding drivers of hydroclimatic variability for robust flood risk planning in the coastal zone. *Australian J Water Resources* 17(2):126–134.
25. Ishak EH, Rahman A, Westra S, Sharma A, Kuczera G (2013) Evaluating the non-stationarity of Australian annual maximum floods. *J Hydrol (Amst)* 494:134–145.
26. Livezey RE, Chen WY (1983) Statistical field significance and its determination by Monte Carlo techniques. *Mon Weather Rev* 111(1):46–59.
27. Ward PJ, Beets W, Bouwer LM, Aerts JCJH, Renssen H (2010) Sensitivity of river discharge to ENSO. *Geophys Res Lett* 37(12):L12402.
28. Ward PJ, Eisner S, Flörke M, Dettinger MD, Kummu M (2014) Annual flood sensitivities to El Niño Southern Oscillation at the global scale. *Hydrol Earth Syst Sci* 18:47–66.
29. Bouma MJ, Kovats RS, Goubet SA, Cox JS, Haines A (1997) Global assessment of El Niño's disaster burden. *Lancet* 350(9089):1435–1438.
30. Dilley M, Heyman BN (1995) ENSO and disaster: Droughts, floods and El Niño/Southern Oscillation warm events. *Disasters* 19(3):181–193.
31. Goddard L, Dilley M (2005) El Niño: Catastrophe or opportunity. *J Clim* 18(5):651–665.
32. Kummu M, Ward PJ, De Moel H, Varis O (2010) Is physical water scarcity a new phenomenon? Global assessment of water shortage over the last two millennia. *Environ Res Lett* 5(3):034006.
33. Tudhope AW, et al. (2001) Variability in the El Niño-Southern Oscillation through a glacial-interglacial cycle. *Science* 291(5508):1511–1517.
34. Cobb KM, et al. (2013) Highly variable El Niño-Southern Oscillation throughout the Holocene. *Science* 339(6115):67–70.
35. Li J, et al. (2013) El Niño modulations over the past seven centuries. *Nat Clim Change* 3:822–826.
36. Verdon-Kidd DC, Franks SW (2006) Long-term behaviour of ENSO: Interactions with the PDO over the past 400 years inferred from paleoclimate records. *Geophys Res Lett* 33(6):L06712.
37. Van Oldenborgh GJ, Philip SY, Collins M (2005) El Niño in a changing climate: A multi-model study. *Ocean Sci* 1:81–95.
38. Paeth H, Scholten A, Friederichs P, Hense A (2008) Uncertainties in climate change prediction: El Niño Southern Oscillation and monsoons. *Global Planet Change* 60(3-4): 265–288.
39. Guilyardi E, et al. (2009) Understanding El Niño in ocean–atmosphere general circulation models. Progress and challenges. *Bull Am Meteorol Soc* 90:325–340.
40. Jongman B, et al. (2014) Increasing stress on disaster-risk finance due to large floods. *Nat Clim Change* 4:264–268.
41. Cheng Y, Tang Y, Chen D (2011) Relationship between predictability and forecast skill of ENSO on various time scales. *J Geophys Res* 116:C12006.
42. Merz B, et al. (2014) Floods and climate: Emerging perspectives for flood risk assessment and management. *Nat Hazard Earth Sys* 2:1559–1612.
43. Coughlan de Perez E, et al. (2014) Forecast-based financing: An approach for catalyzing humanitarian action based on extreme weather and climate forecasts. *Nat Hazard Earth Sys Disc* 2:3193–3218.
44. Braman LM, et al. (2013) Climate forecasts in disaster management: Red Cross flood operations in West Africa, 2008. *Disasters* 37(1):144–164.
45. Pagano TC, Hartmann HC, Sorooshian S (2002) Factors affecting seasonal forecast use in Arizona water management: a case study of the 1997-98 El Niño. *Clim Res* 21: 259–269.
46. GFDRR (2014) *Understanding Risk: The Evolution of Disaster Risk Assessment* (World Bank Global Facility for Disaster Reduction and Recovery, Washington, DC).
47. Van Beek LPH, Wada Y, Bierkens MFP (2011) Global monthly water stress: I. Water balance and water availability. *Water Resources Res* 47(7):W07517.
48. Weedon GP, et al. (2011) Creation of the WATCH forcing data and its use to assess global and regional reference crop evaporation over land during the twentieth century. *J Hydrometeorol* 12(5):823–848.